Environmental Science & Technology

Article

pubs.acs.org/est

Wavelength-Resolved Photon Fluxes of Indoor Light Sources: Implications for HO_x Production

Shawn F. Kowal, Seth R. Allen, and Tara F. Kahan*

1-014 Center for Science and Technology, Syracuse University 111 College Place Syracuse, New York 13244, United States

Supporting Information

ABSTRACT: Photochemistry is a largely unconsidered potential source of reactive species such as hydroxyl and peroxy radicals (OH and HO_2, "HO_x") indoors. We present measured wavelength-resolved photon fluxes and distance dependences of indoor light sources including halogen, incandescent, and compact fluorescent lights (CFL) commonly used in residential buildings; fluorescent tubes common in industrial and commercial settings; and sunlight entering buildings through windows. We use these measurements to predict indoor HO_x production rates from the photolysis of nitrous acid (HONO), hydrogen peroxide (H_2O_2), ozone (O_3), formaldehyde (HCHO), and acetaldehyde (CH_3CHO). Our results suggest that while most lamps can photolyze these molecules, only sunlight and fluorescent tubes will be important to room-averaged indoor HO_x levels due to the strong distance dependence of the fluxes from compact bulbs. Under ambient conditions, we predict that sunlight and fluorescent lights will photolyze HONO to form OH at rates of 10^6–10^7 molecules cm^{-3} s^{-1}, and that fluorescent lights will photolyze HCHO to form HO_2 at rates of ~10^6 molecules cm^{-3} s^{-1}; rates could be 2 orders of magnitude higher under high precursor concentrations. Ozone and H_2O_2 will not be important photochemical OH sources under most conditions, and CH_3CHO will generally increase HO_2 production rates only slightly. We also calculated photolysis rate constants for nitrogen dioxide (NO_2) and nitrate radicals (NO_3) in the presence of the different light sources. Photolysis is not likely an important fate for NO_3 indoors, but NO_2 photolysis could be an important source of indoor O_3.

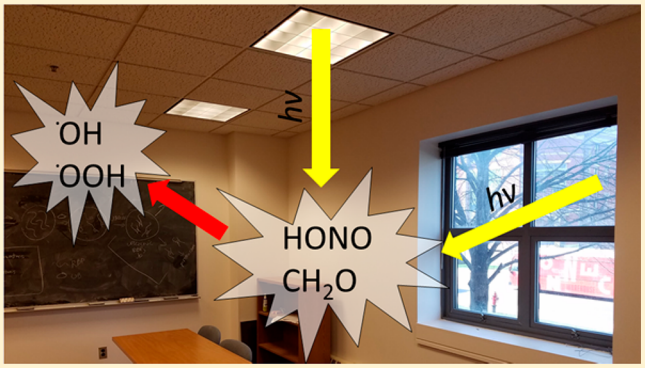

INTRODUCTION

The composition of the outdoor atmosphere is driven by photochemistry. Photolysis of trace gases produces species such as hydroxyl radicals (OH) and peroxy radicals (HO_2). Collectively called "HO_x", these radicals control the oxidizing capacity of the troposphere. HO_x "scrubs" the atmosphere by reacting rapidly and nonselectively with trace gases to produce more oxidized and water-soluble products that are washed out during rain events. Sources and sinks of HO_x are a key theme of atmospheric research.

Much less effort has been devoted to investigating chemistry indoors, despite the fact that people spend over 80% of their time indoors,[1] and indoor air quality is known to affect occupant health (for example, there is an entire body of literature on "sick building syndrome").[2−4] Until the 1990s, indoor air composition was thought to be controlled by air exchange with the outdoors. Despite research in 1986 that described a number of reactions that could alter indoor air composition,[5] it was another ten years before OH production indoors via ozone−alkene reactions was demonstrated experimentally.[6] This mechanism has until very recently been thought to be the only significant OH source indoors.

While radicals such as HO_x are generated primarily through photolysis outdoors, photons with wavelengths shorter than ~400 nm that can initiate photochemistry are largely expected to be absent indoors. However, several researchers have suggested that photochemistry could affect indoor air quality despite the attenuation of UV light, and a recent study demonstrated that sunlight indoors can photolyze nitrous acid (HONO) to form OH.[5,7,8] In fact, under some conditions, HONO photolysis could be the *dominant* indoor OH source. Since then, further studies have reported on the effects of combustion on HONO formation and photochemical OH production, on indoor solar photon fluxes in different locations and at different times, and on the potential for nitrogen dioxide (NO_2) and nitrate radicals (NO_3) to undergo photolysis indoors.[9,10]

Having established that photochemistry can significantly influence indoor air composition, two pressing questions emerge: (1) Can illumination from sources other than sunlight

Received: April 18, 2017
Revised: July 27, 2017
Accepted: August 14, 2017
Published: August 14, 2017

DOI: 10.1021/acs.est.7b02015
Environ. Sci. Technol. 2017, 51, 10423−10430

initiate indoor photochemistry? And (2) can photolysis of species other than HONO contribute to indoor HO_x? With respect to the first question, artificial light sources provide the majority of interior illumination in developed countries. While emission of light bulbs has been well-characterized in the visible region, the same is not true in the UV. The need for such work has not gone unnoticed: There have been several recent calls for characterization of indoor light sources in the actinic region in order to better understand indoor chemistry and air quality.[11−15]

Currently, HONO is the only species that has been shown to photochemically produce HO_x indoors.[7,10,16] However, several other species could be potential photochemical HO_x sources, including ozone (O_3), hydrogen peroxide (H_2O_2), formaldehyde (HCHO), and acetaldehyde (CH_3CHO). In this work we report wavelength-resolved photon fluxes and distance dependences of artificial light sources as well as of sunlight filtered through a window. We also predict photochemical OH and HO_2 production rates indoors due to irradiation of the chemical species listed above by the different light sources. Our results indicate that under some conditions artificial light sources could contribute significantly to indoor HO_x levels, and that species other than HONO may be important indoor photochemical HO_x sources.

MATERIALS AND METHODS

Light Sources. "Soft white" 60 or 60 W equivalent light bulbs ("compact bulbs") were purchased: halogen (GE), incandescent (Electrix), compact fluorescent lightbulb (CFL, Sylvania), and light emitting diode (LED, Osram). Several halogen and CFL light bulbs with different powers were also purchased, as was a GE 3500 K bright white 32 W fluorescent tube. The compact bulbs were placed in a standard light bulb fixture, and the fluorescent tube was placed in a single bulb shop light fixture (Utilitech). Wavelength-resolved photon fluxes (F) were measured at distances from the bulb ranging from 2 mm to 3 m. Photon fluxes from fluorescent tubes were measured in situ in two offices in the Syracuse University chemistry building at distances ranging from 8.2 cm to 1.7 m. Sunlight fluxes were also measured in the chemistry building; details of the sampling sites are provided in the Supporting Information (SI).

Photon Flux Measurements. Light was collected by a 1 m fiber optic cable (Thorlabs) with a cosine corrector attached to an Ocean Optics USB4000 spectrometer. All measurements were acquired with the detector oriented directly toward the light source to maximize light collection. A computer fan was attached to the spectrometer to dissipate heat and improve the signal-to-noise ratio. The spectrometer was calibrated using a DH-2000-CAL lamp (Ocean Optics), and a UVP Pen-Ray PS-1 mercury lamp was used for spectral calibrations. Spectral integration times were set by the instrument software to maximize signal (sunlight ∼1.5 ms, halogen and incandescent ∼4 s, LED ∼3 s, fluorescent bulbs and tubes ∼0.10 ms); 10 scans were averaged for each measurement. Further details about signal processing and error analysis are provided in the SI.

Quality control experiments were performed to ensure that scattered light did not introduce artifacts to our measurements; these are described in the SI. The results indicate that our irradiance measurements capture the vast majority of the total actinic flux, and that any uncertainty in photon fluxes introduced by scattering would be much smaller than that introduced by, e.g., different window composition, bulb types, and (in the case of sunlight) times of day or year.

HO_x Production Rate Calculations. The measured photon flux from each light source was used to calculate photolysis rate constants (J) for the HO_x precursors discussed above:

$$J = \int_{\lambda_i}^{\lambda_f} \sigma(\lambda)\phi(\lambda)F_\lambda \, d\lambda \quad (1)$$

where λ is the wavelength, σ is the absorption cross-section of the molecule, and ϕ is the photolysis quantum yield of the product of interest (Figures S3−S6 in the SI).

We also calculated overtone photolysis rate constants of H_2O_2, in which vibrationally (but not electronically) excited H_2O_2 decomposes after absorbing light at 603 or 615 nm.[17] Overtone photolysis contributed to between 1% and 13% of the total H_2O_2 photolysis rate constant, depending on the light source (except for the LED and covered fluorescent tube, where it accounted for 99% and 65%). The reported H_2O_2 rate constants are the sum of direct and overtone-initiated photolysis rate constants. A full description of the overtone photolysis calculations and results is provided in the SI.

HO_x production rates were calculated from eqs 2−6 using mixing ratios of H_2O_2, HONO, O_3, HCHO, and CH_3CHO relevant to indoor residential environments. A full discussion of the calculations used to arrive at these equations is provided in the SI.

$$\text{rate} = 2J_{H_2O_2}[H_2O_2] \quad (2)$$

$$\text{rate} = J_{HONO}[HONO] \quad (3)$$

$$\text{rate} = 0.19J_{O(^1D)}[O_3] \quad (4)$$

$$\text{rate} = 2J_{rad}[HCHO] \quad (5)$$

$$\text{rate} = J_{rad}[CH_3CHO] \quad (6)$$

We also calculated photolysis rate constants for nitrogen dioxide (NO_2) and nitrate radicals (NO_3). These compounds absorb light at longer wavelengths and have been suggested to photolyze readily indoors.[9] Details are provided in the SI.

RESULTS AND DISCUSSION

Measured Photon Fluxes. Figure 1a shows wavelength-resolved photon fluxes for the compact bulbs; extended spectra and tabulated photon fluxes are provided in Figure S8 and Tables S12 and S13 in the SI. The LED has very little intensity at short wavelengths, with no emission observed below 400 nm. The emission intensity from halogen and incandescent bulbs increases with increasing wavelength; weak emission is observed at wavelengths as short as 300 nm. Emission from the CFL consists of a number of sharp peaks that correspond to mercury emission lines.

Figure 1b shows photon fluxes from a fluorescent tube and from fluorescent lights in two offices. The fluorescent tube has the same spectral features as the CFL shown in Figure 1a, but has an additional broad hump between 300 and 360 nm and a sharp peak at 312 nm. The lights in one office were covered by a plastic shade, while those in the second office were uncovered. Emission from the covered fixture has a similar profile (but lower overall intensity) than that from the CFL, while the uncovered fixture shows the same emission at short wave-

DOI: 10.1021/acs.est.7b02015
Environ. Sci. Technol. 2017, 51, 10423−10430

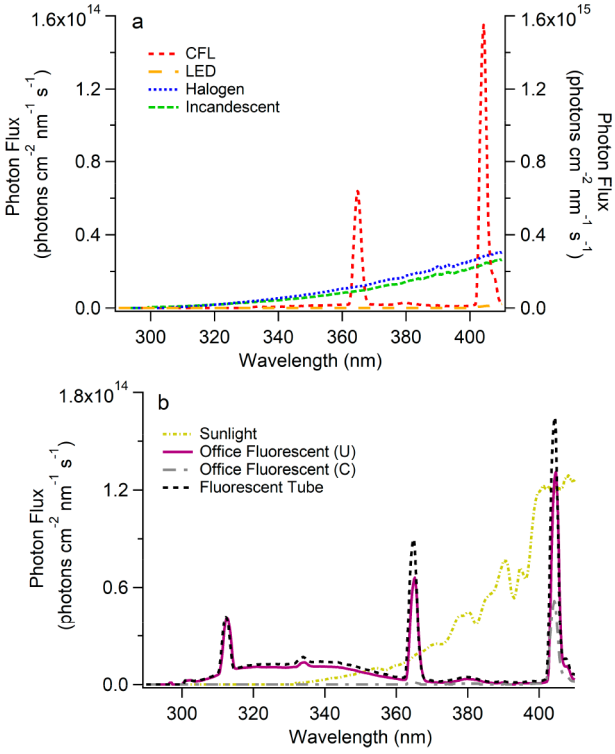

Figure 1. Spectra of (a) 60 W (or equivalent) compact bulbs, and (b) sunlight indoors, fluorescent lights in an office, and a single fluorescent tube between 290 and 410 nm. "U" and "C" refer to office light fixtures that were bare (uncovered) and shaded (covered). The CFL photon flux is plotted on the right *y*-axis of panel (a); fluxes from all other light bulbs are plotted on the left *y*-axis. Photon fluxes from sunlight were measured indoors (Lat. +43.0889, Lon. −76.1545) at noon beside a southward facing window in direct sunlight. Spectra were acquired directly adjacent to the light sources.

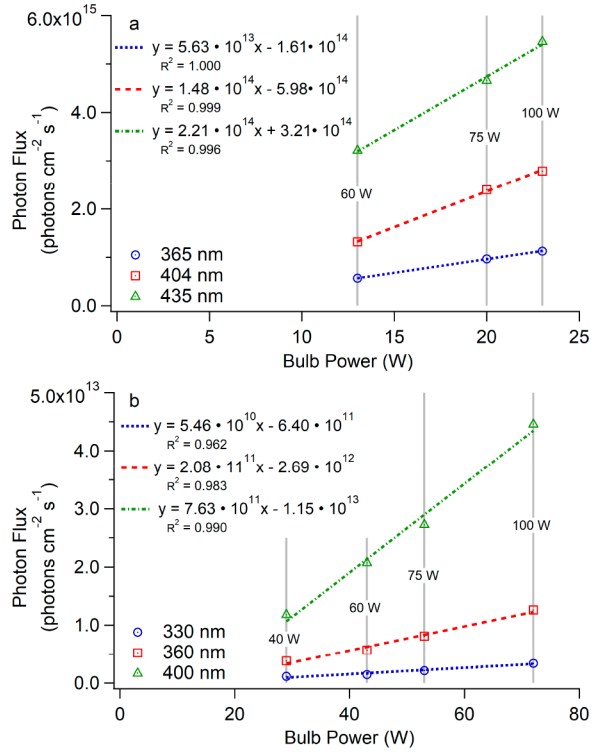

Figure 2. Photon fluxes at individual wavelengths for (a) CFLs and (b) halogen bulbs of different powers. The dashed and dotted traces are linear fits to the data. Vertical solid gray lines show the incandescent bulb equivalent power.

lengths as the individual fluorescent tube shown in Figure 1b. These features likely exist in the CFL and the covered fluorescent tube, but are absorbed by the bulb casing and the plastic cover, respectively. This feature has not to our knowledge been reported previously. To ensure that this emission was real, we acquired spectra of a Philips fluorescent tube with our spectrometer and with an Optronix radiometer. As shown in the SI, the emission at short wavelengths was detected by both spectrometers. We also acquired spectra from three different types of fluorescent tubes. As shown in Figure S9 in the SI, the emission at short wavelengths was observed for all three lights. These features appear, therefore, to be real and not unique to one particular brand of bulb. Figure 1b also shows the wavelength-resolved photon flux from sunlight measured directly in front of a window at noon on February 3, 2015. No penetration was observed indoors at wavelengths shorter than 330 nm, and negligible emission was observed when the detector was not in direct sunlight.

Figure 2 shows photon fluxes at several wavelengths for halogen and CFL bulbs of different powers. LEDs were also analyzed, but emission at wavelengths shorter than 400 nm was not observed, so they are not shown. Photon fluxes increased linearly with power for both halogens and CFLs. The spectral profile of CFL bulbs was the same at all powers tested, while the higher wattage halogen bulbs exhibited emission at shorter wavelengths than those observed for the 60 W equivalent bulb. It is likely that the 60 W bulb also emits at these shorter wavelengths, but that the emission is below the detection limit of our instrument. These results will enable scientists to extrapolate photon fluxes to lamps of different powers.

Distance Dependences. We measured photon fluxes of each light source as a function of distance. Figure 3 shows CFL and fluorescent tube photon fluxes at several wavelengths normalized to the flux near the lamp. Distance dependences for the other lamps are shown in the SI. The dependence for the compact bulbs was d^{-x}, where x ranged from 1.56 to 1.72. This dependence was the same at each wavelength investigated. Photon fluxes from the fluorescent tube varied with $d^{-0.82}$. This deviation from inverse square law for a point source is due to the shape of the bulb.

The uncovered fluorescent light fixtures in the office (shown in the SI) varied with $d^{-0.420}$ in the visible and $d^{-0.603}$ in the ultraviolet. The somewhat poor fit of the data in the UV to a power law is likely due to contributions from the intensity from wavelength-dependent reflection and scattering from the light fixture. The fit captures the intensity relative to that near the source well at most distances, and should introduce only minor uncertainty to distance-dependent photochemical kinetic predictions. Photon fluxes from covered fluorescent tubes in the visible were similar to those from uncovered fluorescent tubes in the UV, with a distance dependence of $d^{-0.629}$; intensity in the UV was too low to acquire a distance dependence. Photon fluxes from fluorescent tubes remained above 10% of original intensity within a distance of 1.3 m from the source, and above 1% within approximately 1.7 m. Figure 3b shows that photon fluxes from sunlight entering a room through a window remained above 90% of the flux measured at the window at distances as great as 2.4 m. In agreement with a previous study, sunlight photon fluxes were largely independent

DOI: 10.1021/acs.est.7b02015
Environ. Sci. Technol. 2017, 51, 10423−10430

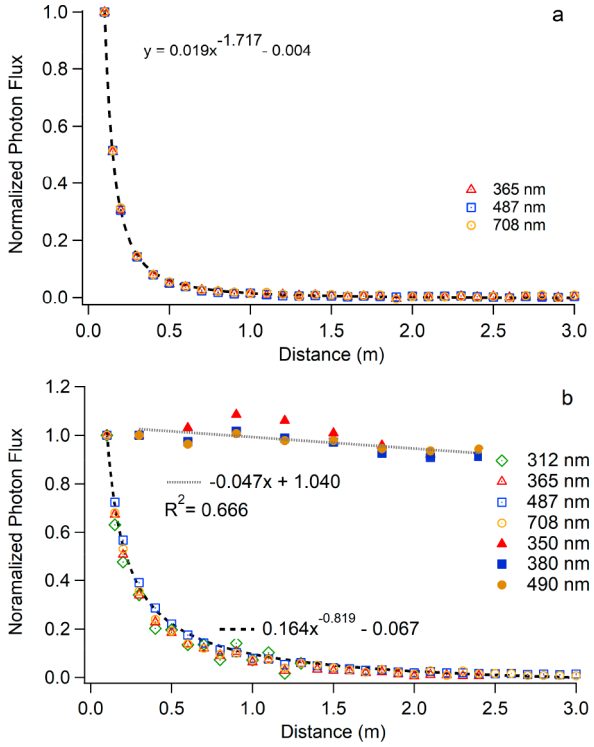

Figure 3. Photon flux as a function of distance normalized to measured flux at 10 cm from the source (for bulbs) or 6.6 cm from the window (sunlight) for (a) a CFL and (b) a fluorescent tube (open symbols) and sunlight (solid symbols). The dashed trace in panel (a) is a fit to the averaged data at the three plotted wavelengths. The dashed trace in panel (b) is a fit to the averaged data of all Hg peaks from the fluorescent fixture between 365 and 708 nm (intensity at 312 nm was too low to acquire a good fit), and the dotted trace is a linear fit to the averaged sunlight data.

of distance from the window because the sun (rather than the window) is the point source; given the distance between the sun and the earth, a change in radius of a few meters will not affect the photon flux.[18]

Predicted Photochemical HO_x Production Rates. HO_x production rates depend on both the photolysis rate constant and the mixing ratio of each precursor molecule. We used literature absorption cross-sections and quantum yields along with measured photon fluxes to calculate photolysis rate constants for H_2O_2, HONO, O_3, HCHO, and CH_3CHO immediately adjacent to indoor light sources (Table S5 in the SI). Table 1 lists expected minimum and maximum indoor mixing ratios of H_2O_2, O_3, HONO, HCHO, and CH_3CHO, as well as a "typical" value that represents a likely indoor mixing ratio in cities during a summer day based on the available literature. Justifications for our selected values are provided in the SI. Table 2 lists photochemical HO_x production rates calculated using eqs 2−6 at typical precursor mixing ratios. HO_x production rates at predicted minimum and maximum indoor precursor concentrations are reported in the SI. The rates listed are those expected directly adjacent to the light source. As discussed above, all of the light sources except for the fluorescent tubes and sunlight depend strongly on distance. We therefore also calculated expected HO_x production rates 1 m away from the source (Table 3). This distance was chosen because an average adult's head will be approximately 0.9 m from the ceiling of a 2.7 m tall room when standing, and 1.2 m from the ceiling when sitting. In a standard 2.4 m tall office, an average human's head will be 0.6 and 0.9 m from the ceiling when standing and sitting, respectively.

Table 1. Expected Indoor Minimum, Maximum, and Typical Mixing Ratios for the HO_x Precursors H_2O_2,[19,20] HONO,[7,21,22] O_3,[23−26] HCHO,[27−29] and CH_3CHO[30−32] Based on Measured and Predicted Values

precursor	minimum (ppb)	maximum (ppb)	typical (ppb)
H_2O_2	0.1	10	1
HONO	0.1	20	5
O_3	0.1	200	20
HCHO	3	600	20
CH_3CHO	1	50	10

Dark HO_x Production Routes Indoors. As discussed in the Introduction, the only indoor OH source that is generally considered to be important is ozone−alkene reactions. For 20 ppb O_3 indoors and typical alkene concentrations, OH is expected to be produced at a rate of ~1.22×10^7 molecules cm^{-3} s^{-1}.[6] Production will be significantly less at night due to lower O_3 concentrations.[33] The primary indoor HO_2 production routes currently considered are physical transport from outdoors (which occurs at a rate of approximately 1.86×10^6 molecules cm^{-3} s^{-1} during the day based on a standard air exchange rate of 1 h^{-1} and 25 ppt HO_2, and is negligible at night due to low outdoor HO_2 levels), and radon decay, which produces HO_2 at a rate of 20.7 molecules cm^{-3} s^{-1} for 48 Bq m^{-3} radon.[34−37] Even at high indoor radon levels (~90 Bq m^{-3}), HO_2 production from radon decay will still be insignificant compared to physical transport.[36] For photochemistry to be an important indoor HO_x source, photochemical HO_x production rates must be competitive with dark production rates.

Photochemical HO_x Production Indoors. As shown in Table 2, LEDs will not initiate significant photochemical HO_x formation under any circumstances, and HO_x production initiated by covered fluorescent tubes will be too slow to be important. Halogens, incandescents, and CFLs are all capable of forming OH and HO_2 (from HONO and HCHO photolysis, respectively) at rates greater than 10% of those from dark processes. This is only true near the light source, however. At average head height, HO_x production from these light sources will be negligible. Fluorescent tubes can initiate HO_x production rates greater than 10% of those from dark sources up to distances of 1 m for OH from HONO photolysis and 1.9 m for HO_2 from HCHO photolysis. HO_x production rates from sunlight will be similar to those near windows in all fully illuminated indoor regions. We therefore focus our discussion on fluorescent tubes and sunlight. The values discussed for fluorescent tubes are for the uncovered fluorescent fixtures in an office, as this is the configuration that is most relevant to actual illumination conditions in buildings. Ozone and H_2O_2 are predicted to be largely unimportant to indoor OH formation; these molecules are discussed in the SI.

Nitrous Acid Photolysis. Previous studies have reported that OH production from HONO photolysis may occur as rapidly as ozone−alkene reactions under some conditions.[7,16] Between 5:00 and 7:00 p.m. in the summer, rates ranging from 0.1 to 2.9×10^7 molecules cm^{-3} s^{-1} were reported in a room containing 1.2 to 3.2×10^{11} molecules cm^{-3} (4.5 to 12 ppb) HONO, illuminated only by sunlight entering through a window.[7] Using our measured solar photon fluxes, we predict a

DOI: 10.1021/acs.est.7b02015
Environ. Sci. Technol. 2017, 51, 10423−10430

Table 2. Predicted Indoor OH Production Rates from H_2O_2, O_3, and HONO Photolysis, and HO_2 Production Rates from HCHO and CH_3CHO Photolysis Directly Adjacent to Different Illumination Sources under Typical Precursor Mixing Ratios

	production rate (molecules cm^{-3} s^{-1})				
	OH			HO_2	
light source	H_2O_2	O_3	HONO	HCHO	CH_3CHO
LED	9.90×10^2	7.44	none	none	none
halogen	1.18×10^4	4.82×10^4	1.05×10^7	7.34×10^5	2.11×10^4
incandescent	1.25×10^4	1.86×10^5	8.52×10^6	9.14×10^5	4.57×10^4
CFL	2.44×10^4	7.40×10^3	4.42×10^7	1.49×10^5	1.03×10^3
fluorescent tube	6.38×10^4	9.05×10^5	1.20×10^7	5.86×10^6	3.54×10^5
office fluorescent (C)[a]	3.50×10^2	9.00×10^1	1.19×10^5	none	none
office fluorescent (U)[a]	5.73×10^4	8.82×10^5	9.51×10^6	5.62×10^6	3.35×10^5
sunlight[b]	7.38×10^3	2.34×10^3	1.70×10^7	6.22×10^3	none

[a]"C" and "U" refer to covered and uncovered fluorescent tubes, respectively. [b]Values assume direct sunlight.

Table 3. Predicted Indoor OH Production Rates from H_2O_2, O_3, and HONO Photolysis, and HO_2 Production Rates from HCHO and CH_3CHO Photolysis 1 m from the Illumination Sources under Typical Precursor Mixing Ratios Based on Measured Distance Dependences

	production rate (molecules cm^{-3} s^{-1})				
	OH			HO_2	
light source	H_2O_2	O_3	HONO	HCHO	CH_3CHO
LED	1.78×10^1	none	none	none	none
halogen	2.59×10^2	1.06×10^3	2.35×10^5	1.61×10^4	4.63×10^2
incandescent	2.74×10^2	4.10×10^3	1.88×10^5	2.01×10^4	1.01×10^3
CFL	3.66×10^2	1.11×10^2	6.63×10^5	2.23×10^3	1.55×10^1
fluorescent tube	2.74×10^3	3.89×10^4	5.17×10^5	2.52×10^5	1.52×10^4
office fluorescent (C)[a]	5.11×10^1	1.31×10^1	1.74×10^4	none	none
office fluorescent (U)[a]	8.43×10^3	1.30×10^5	1.40×10^6	8.26×10^5	4.93×10^4
sunlight[b]	6.64×10^3	2.10×10^3	1.53×10^7	5.60×10^3	none

[a]"C" and "U" refer to covered and uncovered fluorescent tubes, respectively. [b]Values assume direct sunlight.

production rate of 1.5 to 4.0×10^7 molecules cm^{-3} s^{-1} at noon in the winter for the same range of HONO mixing ratios; these rates are in good agreement with the measured rates, despite differences in location, date, and time.[7] Photon fluxes predicted by the Tropospheric Ultraviolet and Visible (TUV) Radiation Model (Figure S15 in the SI) suggest that photon fluxes from direct sunlight (outdoors) during our experiments and those of Gomez Alvarez et al. were similar.[7,38]

Hydroxyl radical production from HONO photolysis initiated by artificial light sources has not been considered. As shown in Tables 2 and 3, we predict OH production rates from HONO photolysis by fluorescent fixtures of 9.5×10^6 molecules cm^{-3} s^{-1} near the lamp and 1.4×10^6 molecules cm^{-3} s^{-1} at a distance of 1 m. If HONO mixing ratios are at the high end of the reported range of measured values, then the predicted OH production rates (provided in the SI) increase to 6.8×10^7 molecules cm^{-3} s^{-1} in the presence of sunlight and 3.8×10^7 molecules cm^{-3} s^{-1} in the presence of fluorescent lights (5.6×10^6 molecules cm^{-3} s^{-1} 1 m away). Production rates from sunlight are similar to those from ozone alkene reactions at typical HONO concentrations, and up to 6× greater at high concentrations. Rates from fluorescent tubes will be similar to dark rates near the lamp at ambient concentrations and ∼10% of dark rates 1 m away. At high concentrations the rate will increase to 50−300% of the dark rate depending on the distance from the bulb. Our results support previous claims that HONO photolysis can be an important indoor OH source, and show that this may be the case even in the absence of sunlight.

Formaldehyde Photolysis. For HCHO photolysis to be an important indoor HO_2 source, HO_2 production rates must be on the same order of magnitude as physical transport (1.86×10^6 molecules cm^{-3} s^{-1}).[39] At a typical indoor HCHO mixing ratio of 20 ppb, we predict that HO_2 production rates from photolysis by fluorescent lights will be similar to that from physical transport even at a distance of 1 m from the bulb, while the production rate due to sunlight is predicted to be 0.3% of that from physical transport. At high HCHO mixing ratios (on the order of 600 ppb) photolysis will be the dominant indoor HO_2 source under illumination from fluorescent lights, with predicted rates of 1.7×10^8 molecules cm^{-3} s^{-1} near the light fixture and 2.5×10^7 molecules cm^{-3} s^{-1} at 1 m. At high concentrations sunlight will photolyze HCHO to form HO_2 at a rate of 1.7×10^5 molecules cm^{-3} s^{-1}, which is ∼10% of the rate from physical transport.

Acetaldehyde Photolysis. At typical indoor aldehyde concentrations, HO_2 production from acetaldehyde photolysis will be 6% that from formaldehyde photolysis. Acetaldehyde is therefore not expected to be an important source of HO_x under ambient conditions, but it will contribute slightly to HO_2 production rates. In indoor spaces with high human occupancy, CH_3CHO levels will increase relative to HCHO levels, and acetaldehyde's contribution to indoor HO_2 levels will become more important.

Nighttime HO_x Production. At night, outdoor OH and O_3 levels are very low, and, with some exceptions, dark indoor OH production rates are expected to be negligible.[33,39] Further, the absence of sunlight means that photochemistry will be

DOI: 10.1021/acs.est.7b02015
Environ. Sci. Technol. 2017, 51, 10423−10430

restricted to reactions initiated by artificial light sources. If nighttime indoor HONO levels are similar to daytime levels, HONO photolysis will likely be the only important indoor OH source under these conditions. Diurnal NO_2 profiles have been reported in a commercial building, with daytime maxima ranging from 10 to 40 ppb, and nighttime minima ranging from 1 to 15 ppb.[33,40] Different diurnal profiles may be observed in residential buildings, where combustion (for example from cooking) will increase NO_2 mixing ratios in the evenings when people are generally at home, thereby increasing HONO levels. HONO photolysis may therefore be an important OH source even at night. Physical transport is a negligible source of indoor HO_2 at night, and production from radon decay is very small, so we predict that HCHO photolysis (with minor contributions from CH_3CHO) will be the only significant indoor HO_2 source at night.[39]

HO_x Production Near Light Sources. As discussed above, only fluorescent tubes and sunlight are expected to affect room-averaged HO_x levels due to the strong distance dependence of emission from the other light sources. However, some of these light sources may create elevated *local* HO_x mixing ratios in the vicinity of the light source. For example, OH and HO_2 from HONO and HCHO photolysis near halogen, incandescent, and CFL bulbs are predicted to form at similar rates as dark production methods at ambient precursor concentrations. People often spend time in close proximity to artificial light sources, for example when eating dinner (with illumination from a dining room chandelier) or reading or working (with illumination from a desk or floor lamp). In confined spaces, such as prefab trailers, people will be on average even closer to light sources. Given the high formaldehyde concentrations measured in prefab trailers, this could lead to significant HO_x mixing ratios near head height in these spaces.

Photolysis of NO_2 and NO_3. While the focus of this work was on species that photolyze to form HO_x, other photochemical reactions may be important to indoor air quality. For example, NO_2 photolysis forms O_3, and NO_3 is an important oxidant outdoors at night when HO_x levels are low.[41] Photolysis rate constants for these species have recently been calculated for illumination by sunlight indoors.[9] We calculated photolysis rate constants due to different light sources (Table S10 in the SI). Our predicted NO_2 photolysis rate constant from sunlight of 1.4×10^{-3} s^{-1} is in excellent agreement with that of Gandolfo et al. ($(1.41 \pm 0.10) \times 10^{-3}$ s^{-1} in the summer), and slightly higher than the rate constants reported by Gomez Alvarez et al. ($\sim 7 \times 10^{-4}$ s^{-1}).[7,9] The rate constant from fluorescent light fixtures is ~30% of that from sunlight near the lamp, and decreases to ~4% at a distance of 1 m. Ozone production via NO_2 photolysis is therefore likely only important in sunlit regions indoors. For 25 ppb NO_2 indoors we predict an O_3 production rate of 1.9×10^9 molecules cm^{-3} s^{-1}.[21,33,40,42] This could increase indoor O_3 levels by a factor of 5 compared to levels expected based only on physical transport from outdoors (3.8×10^8 molecules cm^{-3} s^{-1} for an air exchange rate of 1 h^{-1} and an outdoor O_3 concentration of 50 ppb) in a fully sunlit room.

We calculated NO_3 photolysis rate constants of 7.6×10^{-2} s^{-1} (to generate NO_2 and $O(^3P)$) and 9.3×10^{-3} s^{-1} (to generate NO and O_2) in the presence of sunlight; rate constants due to fluorescents were ~50% and ~80% of those from sunlight near the lamp, and were ~7% and 12% 1 m away. Our rate constants calculated in sunlight were in agreement with those measured by Gandolfo et al. in summer ($(7.48 \pm 0.37) \times 10^{-2}$ s^{-1} to form NO_2 and $(9.22 \pm 0.46) \times 10^{-3}$ s^{-1} to form NO).[9] We calculated a photolysis lifetime of 12 s in sunlight (Table S11); this is similar to that for reaction with NO (16 s for 10 ppb NO), but much longer than that expected due to reactions with monoterpenes (<1 s).[43−47] Any NO_3 formed indoors will be rapidly titrated by organics, and we do not expect photolysis to be an important fate.

Atmospheric Implications. The wavelength-resolved photon fluxes and distance dependences of common light sources that we report are needed to accurately account for photochemistry in indoor chemistry models. Our calculated HO_x production rates support previous reports that HONO photolysis initiated by sunlight will be an important indoor OH source, and further suggest that HCHO photolysis will be an important indoor HO_2 source. They also indicate that light sources other than sunlight—especially fluorescent tubes—may initiate photochemical HO_x production indoors.

Our results demonstrate that small changes in lighting conditions may greatly alter the oxidizing capacity of indoor spaces. For example, the striking difference in predicted HO_x production rates from covered and uncovered fluorescent tubes suggests that indoor HO_x levels may be significantly reduced simply by covering light fixtures. Our results also suggest that localized HO_x levels (near lamps) indoors may change as incandescent bulbs are phased out in many countries.

The implications of elevated indoor HO_x levels on indoor air quality and human health are unclear. Oxidation may help remove organic species from the air, but the oxidized products may be more harmful than the unoxidized precursors. For example, aldehydes, ketones, and organic and inorganic acids, which are likely products of reactions indoors initiated by HO_x,[48−52] can be airway irritants.[53−56] Hydroxyl radicals can also react with common indoor pollutants such as polybrominated diphenyl ethers (PBDEs), forming more toxic products such as dioxins.[57] Finally, reactions between HO_x and organic molecules such as α-pinene and δ-limonene may contribute to the formation and growth of aerosols, which are associated with negative health effects.[58−60] This work indicates a need for future studies to quantify indoor HO_x production rates from various precursor molecules and light sources, to measure HO_x levels indoors, and to investigate the effects of elevated indoor HO_x levels on air quality and human health.

■ ASSOCIATED CONTENT

Supporting Information

The Supporting Information is available free of charge on the ACS Publications website at DOI: 10.1021/acs.est.7b02015.

Description of indoor measurement sites, instrument validation and uncertainty calculations, absorption cross sections and quantum yields, kinetics calculations, distance dependences, HO_x production rates at low and high precursor concentrations, and wavelength resolved photon fluxes (PDF)

■ AUTHOR INFORMATION

Corresponding Author

*Phone: (315) 443-3285; fax: (315) 443-4070; e-mail: tfkahan@syr.edu.

ORCID

Tara F. Kahan: 0000-0001-5074-1155

Notes

The authors declare no competing financial interest.

DOI: 10.1021/acs.est.7b02015
Environ. Sci. Technol. 2017, 51, 10423−10430

■ ACKNOWLEDGMENTS

This work was supported by funding from an Oak Ridge Associated Universities (ORAU) Ralph E. Powe Junior Faculty Enhancement Award, NSF award CHE-1659775, and Syracuse University. The authors thank Drs. J. P. Hassett and D. J. Kieber for use of instrumentation and helpful discussions, and Dr. C. J. Weschler for helpful discussions and for offering comments on the manuscript prior to submission.

■ REFERENCES

(1) Klepeis, N. E.; Nelson, W. C.; Ott, W. R.; Robinson, J. P.; Tsang, A. M.; Switzer, P.; Behar, J. V.; Hern, S. C.; Engelmann, W. H. The national human activity pattern survey (NHAPS): a resource for assessing exposure to environmental pollutants. *J. Exposure Anal. Environ. Epidemiol.* **2001**, *11* (3), 231−252.

(2) Engvall, K.; Norrby, C.; Norback, D. Sick building syndrome in relation to building dampness in multi-family residential buildings in Stockholm. *Int. Arch. Occup. Environ. Health* **2001**, *74* (4), 270−278.

(3) Muzi, G.; dell'Omo, M.; Abbritti, G.; Accattoli, P.; Fiore, M. C.; Gabrielli, A. R. Objective assessment of ocular and respiratory alterations in employees in a sick building. *Am. J. Ind. Med.* **1998**, *34* (1), 79−88.

(4) Yu, C. W. F.; Kim, J. T. Building pathology, investigation of sick buildings - VOC emissions. *Indoor Built Environ.* **2010**, *19* (1), 30−39.

(5) Nazaroff, W. W.; Cass, G. R. Mathematical modeling of chemically reactive pollutants in indoor air. *Environ. Sci. Technol.* **1986**, *20* (9), 924−934.

(6) Weschler, C. J.; Shields, H. C. Production of the hydroxyl radical in indoor air. *Environ. Sci. Technol.* **1996**, *30* (11), 3250−3258.

(7) Alvarez, E. G.; Amedro, D.; Afif, C.; Gligorovski, S.; Schoemacker, C.; Fittschen, C.; Doussin, J.; Wortham, H. Unexpectedly high indoor hydroxyl radical concentrations associated with nitrous acid. *Proc. Natl. Acad. Sci. U. S. A.* **2013**, *110* (33), 13294−13299.

(8) Carslaw, N. A new detailed chemical model for indoor air pollution. *Atmos. Environ.* **2007**, *41* (6), 1164−1179.

(9) Gandolfo, A.; Gligorovski, V.; Bartolomei, V.; Tlili, S.; Alvarez, E. G.; Wortham, H.; Kleffmann, J.; Gligorovski, S. Spectrally resolved actinic flux and photolysis frequencies of key species within an indoor environment. *Build. Environ.* **2016**, *109*, 50−57.

(10) Bartolomei, V.; Gomez Alvarez, E.; Wittmer, J.; Tlili, S.; Strekowski, R.; Temime-Roussel, B.; Quivet, E.; Wortham, H.; Zetzsch, C.; Kleffmann, J.; Gligorovski, S. Combustion processes as a source of high levels of indoor hydroxyl radicals through the photolysis of nitrous acid. *Environ. Sci. Technol.* **2015**, *49* (11), 6599−6607.

(11) Carslaw, N.; Wolkoff, P. A new European initiative for indoor air pollution research. *Indoor Air* **2006**, *16* (1), 4−6.

(12) Gligorovski, S.; Weschler, C. J. The oxidative capacity of indoor atmospheres. *Environ. Sci. Technol.* **2013**, *47* (24), 13905−13906.

(13) Nazaroff, W. W. Illumination, lighting technologies, and indoor environmental quality. *Indoor Air* **2014**, *24* (3), 225−226.

(14) Weschler, C. J. Chemistry in indoor environments: 20 years of research. *Indoor Air* **2011**, *21* (3), 205−218.

(15) Corsi, R. L. Connect or stagnate: the future of indoor air sciences. *Indoor Air* **2015**, *25* (3), 231−234.

(16) Gligorovski, S.; Wortham, H.; Kleffmann, J. The hydroxyl radical (OH) in indoor air: Sources and implications. *Atmos. Environ.* **2014**, *99*, 568−570.

(17) Brown, S. S.; Wilson, R. W.; Ravishankara, A. R. Absolute intensities for third and fourth overtone absorptions in HNO_3 and H_2O_2 measured by cavity ring down spectroscopy. *J. Phys. Chem. A* **2000**, *104* (21), 4976−4983.

(18) Lim, H. S.; Kim, G. Spectral Characteristics of UV Light Existing in Indoor Visual Environment. *Indoor Built Environ.* **2010**, *19* (5), 586−591.

(19) Fan, Z. H.; Weschler, C. J.; Han, I. K.; Zhang, J. F. Co-formation of hydroperoxides and ultra-fine particles during the reactions of ozone with a complex VOC mixture under simulated indoor conditions. *Atmos. Environ.* **2005**, *39* (28), 5171−5182.

(20) Li, T. H.; Turpin, B. J.; Shields, H. C.; Weschler, C. J. Indoor hydrogen peroxide derived from ozone/d-limonene reactions. *Environ. Sci. Technol.* **2002**, *36* (15), 3295−3302.

(21) Lee, K.; Xue, X. P.; Geyh, A. S.; Ozkaynak, H.; Leaderer, B. P.; Weschler, C. J.; Spengler, J. D. Nitrous acid, nitrogen dioxide, and ozone concentrations in residential environments. *Environ. Health Persp.* **2002**, *110* (2), 145−149.

(22) Pitts, J. N.; Wallington, T. J.; Biermann, H. W.; Winer, A. M. Identification and measurement of nitrous acid in an indoor environment. *Atmos. Environ.* **1985**, *19* (5), 763−767.

(23) Britigan, N.; Alshawa, A.; Nizkorodov, S. A. Quantification of ozone levels in indoor environments generated by ionization and ozonolysis air purifiers. *J. Air Waste Manage. Assoc.* **2006**, *56* (5), 601−610.

(24) Hubbard, H. F.; Coleman, B. K.; Sarwar, G.; Corsi, R. L. Effects of an ozone-generating air purifier on indoor secondary particles in three residential dwellings. *Indoor Air* **2005**, *15* (6), 432−444.

(25) Phillips, T. J.; Bloudoff, D. P.; Jenkins, P. L.; Stroud, K. R. Ozone emissions from a "personal air purifier". *J. Exposure Anal. Environ. Epidemiol.* **1999**, *9* (6), 594−601.

(26) Weschler, C. J. Ozone in indoor environments: Concentration and chemistry. *Indoor Air* **2000**, *10* (4), 269−288.

(27) Hodgson, A. T.; Rudd, A. F.; Beal, D.; Chandra, S. Volatile organic compound concentrations and emission rates in new manufactured and site-built houses. *Indoor Air* **2000**, *10* (3), 178−192.

(28) Liu, W.; Zhang, J.; Zhang, L.; Turpin, B. J.; Weisel, C. P.; Morandi, M. T.; Stock, T. H.; Colome, S.; Korn, L. R. Estimating contributions of indoor and outdoor sources to indoor carbonyl concentrations in three urban areas of the United States. *Atmos. Environ.* **2006**, *40* (12), 2202−2214.

(29) Salthammer, T.; Mentese, S.; Marutzky, R. Formaldehyde in the indoor environment. *Chem. Rev.* **2010**, *110* (4), 2536−2572.

(30) Duan, H. Y.; Liu, X. T.; Yan, M. L.; Wu, Y. T.; Liu, Z. R. Characteristics of carbonyls and volatile organic compounds (VOCs) in residences in Beijing, China. *Front. Environ. Sci. Eng.* **2016**, *10* (1), 73−84.

(31) Chan, W. R.; Cohn, S.; Sidheswaran, M.; Sullivan, D. P.; Fisk, W. J. Contaminant levels, source strengths, and ventilation rates in California retail stores. *Indoor Air* **2015**, *25* (4), 381−392.

(32) Logue, J. M.; McKone, T. E.; Sherman, M. H.; Singer, B. C. Hazard assessment of chemical air contaminants measured in residences. *Indoor Air* **2011**, *21* (2), 92−109.

(33) Weschler, C. J.; Shields, H. C.; Naik, D. V. Indoor chemistry involving O_3, NO, and NO_2 as evidenced by 14 months of measurement at a site in southern California. *Environ. Sci. Technol.* **1994**, *28* (12), 2120−2132.

(34) Baixeras, C.; Climent, H.; Font, L. L.; Bacmeister, G. U.; Albarracin, D.; Monnin, M. M. Using SSNTDs in soil and indoors in two Mediterranean locations for radon concentration measurements. *Radiat. Meas.* **1997**, *28* (1−6), 713−716.

(35) Ding, H. L.; Hopke, P. K. HO_x production due to radon decay in air. *J. Atmos. Chem.* **1993**, *17* (4), 375−390.

(36) Font, L.; Baixeras, C. The RAGENA dynamic model of radon generation, entry and accumulation indoors. *Sci. Total Environ.* **2003**, *307* (1−3), 55−69.

(37) Stone, D.; Whalley, L. K.; Heard, D. E. Tropospheric OH and HO2 radicals: field measurements and model comparisons. *Chem. Soc. Rev.* **2012**, *41* (19), 6348−6404.

(38) Madronich, S. Implications of recent total atmospheric ozone measurements for biologically active ultraviolet radiation reaching the earths surface. *Geophys. Res. Lett.* **1992**, *19* (1), 37−40.

(39) Smith, S. C.; Lee, J. D.; Bloss, W. J.; Johnson, G. P.; Ingham, T.; Heard, D. E. Concentrations of OH and HO_2 radicals during NAMBLEX: measurements and steady state analysis. *Atmos. Chem. Phys.* **2006**, *6*, 1435−1453.

DOI: 10.1021/acs.est.7b02015
Environ. Sci. Technol. 2017, 51, 10423−10430

(40) Challoner, A.; Gill, L. Indoor/outdoor air pollution relationships in ten commercial buildings: $PM_{2.5}$ and NO_2. *Build. Environ.* **2014**, *80*, 159−173.
(41) Finlayson-Pitts, B. J. P. J. N. *Chemistry of the Upper and Lower Atmosphere Theory, Experiments and Applications*; Academic Press: San Diego, CA, 2000.
(42) Weschler, C. J.; Brauer, M.; Koutrakis, P. Indoor ozone and nitrogen dioxide: A potential pathway to the generation of nitrate radicals, dinitrogen pentaoxide, and nitric acid indoors. *Environ. Sci. Technol.* **1992**, *26* (1), 179−184.
(43) Geyer, A.; Alicke, B.; Ackermann, R.; Martinez, M.; Harder, H.; Brune, W.; di Carlo, P.; Williams, E.; Jobson, T.; Hall, S.; Shetter, R.; Stutz, J. Direct observations of daytime NO_3: Implications for urban boundary layer chemistry. *J. Geophys. Res.* **2003**, *108* (D12), 11.
(44) Atkinson, R.; Baulch, D. L.; Cox, R. A.; Crowley, J. N.; Hampson, R. F.; Hynes, R. G.; Jenkin, M. E.; Rossi, M. J.; Troe, J. Evaluated kinetic and photochemical data for atmospheric chemistry: Volume I - gas phase reactions of O_x, HO_x, NO_x and SO_x species. *Atmos. Chem. Phys.* **2004**, *4*, 1461−1738.
(45) Atkinson, R.; Baulch, D. L.; Cox, R. A.; Crowley, J. N.; Hampson, R. F.; Hynes, R. G.; Jenkin, M. E.; Rossi, M. J.; Troe, J. Evaluated kinetic and photochemical data for atmospheric chemistry: Volume II - gas phase reactions of organic species. *Atmos. Chem. Phys.* **2006**, *6*, 3625−4055.
(46) Stutz, J.; Wong, K. W.; Lawrence, L.; Ziemba, L.; Flynn, J. H.; Rappengluck, B.; Lefer, B. Nocturnal NO3 radical chemistry in Houston, TX. *Atmos. Environ.* **2010**, *44* (33), 4099−4106.
(47) Atkinson, R. Kinetics and mechanisms of the gas phase reactions of the NO_3 radical with organic compounds. *J. Phys. Chem. Ref. Data* **1991**, *20* (3), 459−507.
(48) Bloss, C.; Wagner, V.; Jenkin, M. E.; Volkamer, R.; Bloss, W. J.; Lee, J. D.; Heard, D. E.; Wirtz, K.; Martin-Reviejo, M.; Rea, G.; Wenger, J. C.; Pilling, M. J. Development of a detailed chemical mechanism (MCMv3.1) for the atmospheric oxidation of aromatic hydrocarbons. *Atmos. Chem. Phys.* **2005**, *5*, 641−664.
(49) Jenkin, M. E.; Saunders, S. M.; Pilling, M. J. The tropospheric degradation of volatile organic compounds: A protocol for mechanism development. *Atmos. Environ.* **1997**, *31* (1), 81−104.
(50) Jenkin, M. E.; Saunders, S. M.; Wagner, V.; Pilling, M. J. Protocol for the development of the Master Chemical Mechanism, MCM v3 (Part B): tropospheric degradation of aromatic volatile organic compounds. *Atmos. Chem. Phys.* **2003**, *3*, 181−193.
(51) Jenkin, M. E.; Young, J. C.; Rickard, A. R. The MCM v3.3.1 degradation scheme for isoprene. *Atmos. Chem. Phys.* **2015**, *15* (20), 11433−11459.
(52) Saunders, S. M.; Jenkin, M. E.; Derwent, R. G.; Pilling, M. J. Protocol for the development of the Master Chemical Mechanism, MCM v3 (Part A): tropospheric degradation of non-aromatic volatile organic compounds. *Atmos. Chem. Phys.* **2003**, *3*, 161−180.
(53) WHO. *Environmental Health Criteria 167: Acetaldehyde*; World Health Organization: 1995.
(54) WHO. *Environmental Health Criteria 207: Acetone*; World Health Organization: 1998.
(55) WHO. *Environmental Health Criteria 191: Acryllic Acid*; World Health Organization: 1997.
(56) WHO. *Environmental Health Criteria 174: Isophorene*; World Health Organization: 1995.
(57) Erickson, P. R.; Grandbois, M.; Arnold, W. A.; McNeill, K. Photochemical formation of brominated dioxins and other products of concern from hydroxylated polybrominated diphenyl ethers (OH-PBDEs). *Environ. Sci. Technol.* **2012**, *46* (15), 8174−8180.
(58) Dockery, D. W.; Pope, C. A.; Xu, X. P.; Spengler, J. D.; Ware, J. H.; Fay, M. E.; Ferris, B. G.; Speizer, F. E. An association between air pollution and mortality in 6 United States cities. *N. Engl. J. Med.* **1993**, *329* (24), 1753−1759.
(59) Schulz, H.; Harder, V.; Ibald-Mulli, A.; Khandoga, A.; Koenig, W.; Krombach, F.; Radykewicz, R.; Stampfl, A.; Thorand, B.; Peters, A. Cardiovascular effects of fine and ultrafine particles. *J. Aerosol Med.* **2005**, *18* (1), 1−22.
(60) Larsen, B. R.; Di Bella, D.; Glasius, M.; Winterhalter, R.; Jensen, N. R.; Hjorth, J. Gas-phase OH oxidation of monoterpenes: Gaseous and particulate products. *J. Atmos. Chem.* **2001**, *38* (3), 231−276.

DOI: 10.1021/acs.est.7b02015
Environ. Sci. Technol. 2017, 51, 10423−10430